DOI: 10.13009/EUCASS2017-376

DOI:

Computational Ground Effect Aerodynamics and Airplane Stability Analysis During Take-off and Landing

M.Sereez, N.B.Abramov and M.G.Goman
De Montfort University, Leicester, UK
mohamedshereez@gmail.com · nikolay.abramov@dmu.ac.uk · mgoman@dmu.ac.uk
†M.Sereez

Abstract

Computational simulations of aerodynamic characteristics of the Common Research Model (CRM), representing a typical transport airliner, are conducted using CFD methods in close proximity to the ground. The obtained dependencies on bank angle for aerodynamic forces and moments are further used in stability and controllability analysis of the lateral-directional aircraft motion. Essential changes in the lateral-directional modes in close proximity to the ground have been identified. For example, with approach to the ground, the roll subsidence and spiral eigenvalues are merging creating the oscillatory Roll-Spiral mode with quite significant frequency. This transformation of the lateral-directional dynamics in piloted simulation may affect the aircraft responses to external crosswind, modify handling quality characteristics and improve realism of crosswind landing.

1. Introduction

According to statistics of fatal accidents worldwide for commercial Jet Fleet during the period 2006 − 2015 presented by Boeing Company Ltd the number of fatalities during landing due to Abnormal Runway Contact (ARC) and Runway Excursion (RE) holds the second place with controlled flight into terrain (CFIT) after the Loss-of-Control in Flight (LOC-I).[1] Approach and landing accident reduction (ALAR) is the primary goal of the Flight Safety Foundation (FSF).[2] It is noted that a better knowledge of flight dynamics in close proximity to the ground can provide increased understanding of the various crosswind handling techniques to increase safety during a crosswind landing.[2]

Aircraft aerodynamic characteristics and dynamic behaviour are subjected to changes in proximity to the ground during landing approach and take-off flight.[4] An increase in the lift force, reduction in the amount of induced drag, onset of the pitching down moment requires control actions from the pilot for retrimming aircraft. The above mentioned aerodynamic changes due to ground effect in the aircraft longitudinal dynamics and control are well recognised. Special wind tunnel techniques are used for evaluation of the ground effect in the longitudinal aerodynamic characteristics.[5] An analytical study of the ground effect on the airplane longitudinal stability can be found, for example, in paper.[12]

During crosswind landing and take-off the aircraft lateral-directional dynamics can be excited. Aircraft can be approaching and landing with sideslip and nonzero bank angle, this requires levelling aircraft in close proximity to the runway. Therefore the effect of closeness to the ground on the lateral-directional aerodynamic characteristics in such situations should be seriously evaluated. To the best knowledge of the authors, changes in the lateral-directional airplane dynamics due to ground effect have not been addressed in the aeronautical literature and not introduced in the flight simulation practice.

In this paper we approach the above problem by using CFD methods for computational prediction of airplane aerodynamic characteristics in static conditions, when the airplane is flying above the runway with nonzero bank angle. The Common Research Model (CRM)[7,8] of a generic modern transport airplane was considered in its cruise configuration. The CFD simulations were conducted using ANSYS Fluent and OpenFOAM open source software.[11] Most of the previously reported CFD simulations of aerodynamics in ground effect have been carried out for two dimensional airfoils and low aspect ratio configurations.[3,6,9,14]

The ground effect in the CRM aerodynamic forces and moments dependencies has been identified in the CFD simulations and the obtained aerodynamic data were applied for stability and controllability analysis in the lateral-directional airplane motion. The performed dynamic analysis for a typical transport airliner showed transformation of the airplane lateral-directional modes of motion. For example, the roll subsidence and spiral eigenvalues in close proximity to the ground are merging creating the oscillatory Roll-Spiral mode with quite significant frequency. This trans-

DOI: 10.13009/EUCASS2017-376

formation of the lateral-directional dynamics introduced in piloted simulation may affect the flight simulator motion-cueing and handling quality characteristics. The major factor of the performed ground effect dynamic analysis was the introduction of the rolling and yawing moments dependencies on the airplane bank angle, which was equivalent to the "aerodynamic banking stiffness". The airplane responses to ailerons and rudder control inputs also change in close proximity to the ground.

The formulation of the computational framework and simulation results for CRM ground effect aerodynamics are presented in section 2. Section 3 discusses the results of dynamic analysis of the lateral-directional motion and the 6-DOF simulations of the full scale flight simulation model in close proximity to the ground.

2. CFD simulation of ground effect aerodynamics

For evaluation of the ground effect aerodynamics in this study the Common Research Model (CRM) geometry of a generic airliner was selected. This geometry of CRM in wing-body-horizontal tail configuration is available on NASA repository for Drag Prediction Workshop.[7] The geometry is then modified to include the ONERA vertical fin available at.[8] The reference area for CRM model, shown in Fig.1, is $S_{ref} = 383.7m^2$ and $C_{ref} = 7m$, the wing has an aspect ratio of $AR = 9.0$.

Figure 1: Full configuration of the Common Research Model (CRM).

2.1 Grid generation

The build topology of the CRM model has been checked and corrected to ensure air tightness on the model surfaces. After this procedure a hexahedral type of mesh was generated for the full model. A structured mapped blocking approach with appropriate splits and inclusion of O-grids was used to better capture the boundary layer regions on the airplane surfaces.

The blocks initially generated, were transformed through rotations and translations to generate hexahedral unstructured meshes according to flight conditions, i.e. airplane attitude and closeness to the ground. The boundary conditions on the ground were implemented as a moving wall with direction and velocity magnitude of incoming flow and were resolved with inclusion of H-grid layers with appropriate wall distance (Y+<1).

The initial meshes were generated for different altitudes above the ground $h = 4\bar{c}$, $h = 2\bar{c}$, $h = 1\bar{c}$, and $h = 0.5\bar{c}$. At each altitude h the grid was adapted for a number of different angles of attack settings $\alpha = 4, 8, 12°$. At altitude $h = 0.5\bar{c}$ additionally a number of bank angle settings was considered $\phi = 4, 8, 12°$ with additional adaptation of the grid. Fig. 2 shows different CRM attitudes at $h = 0.5\bar{c}$ (different colors are used to highlight different aerodynamic surfaces of the model). The blue mesh in the bottom represents the ground.

The numerical simulations were carried out within reasonable accuracy of a grid between coarse to medium, i.e. 10million cells for a full configuration. This seems suitable for our purpose here to evaluate ground effect.

2.2 Governing equations and boundary conditions

The Navier-Stokes equations governing fluid flow are:

$$\frac{\partial \rho}{\partial t} + \nabla \cdot (\rho u) = 0 \tag{1}$$

$$\frac{\partial u}{\partial t} + (u \cdot \nabla)u - \nu \nabla^2 u = -\nabla p/\rho \tag{2}$$

For the Reynolds numbers typical for industrial applications, the computational resources required for a Direct Numerical Simulation (DNS) of equations (1),(2) are exceeding the currently available technical capabilities. The effect

DOI: 10.13009/EUCASS2017-376

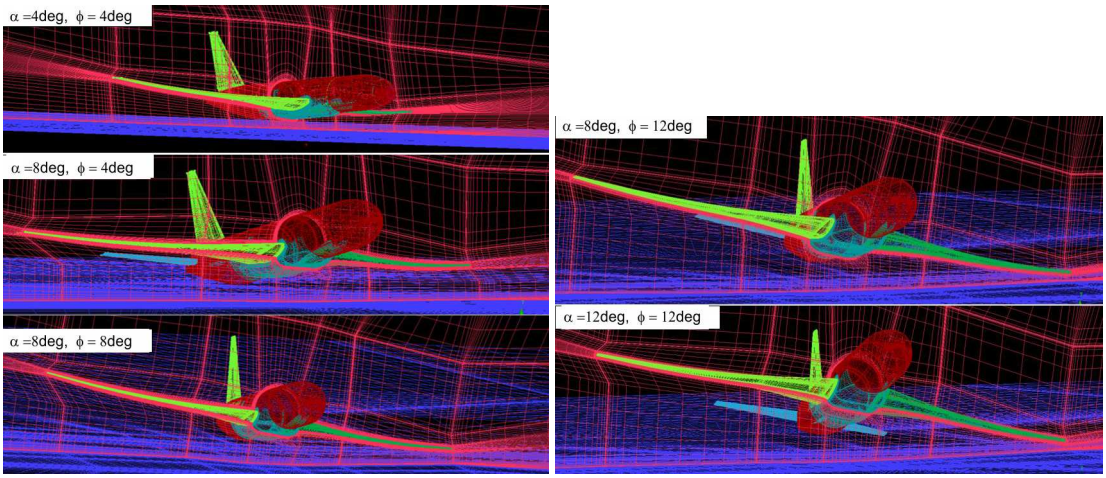

Figure 2: Generated meshes and flight settings.

of turbulence is normally simplified by solving the Reynolds-averaged Navier-Stokes (RANS) equations, which are the time averaged approximation of equations (1),(2). The averaging of fluctuating velocities generates additional terms, known as the Reynolds stresses. To describe these stresses the additional empirical equations, generally differential ones, are required to close the computational model. The majority of RANS models are based on the concept of an eddy viscosity, equivalent to the kinematic viscosity of the fluid, that describes the turbulent mixing or the diffusion of momentum. For closure, the turbulence k-ω SST formulation is used which is commonly used in computational aerodynamic simulations:[10]

$$\frac{\partial \rho k}{\partial t} + \frac{\partial u_j k}{\partial x_j} = G - \beta^\star \rho \omega k + \frac{\partial}{\partial x_j}\left[(\mu + \sigma_k \nu_t)\frac{\partial k}{\partial t}\right] \tag{3}$$

$$\frac{\partial \rho \omega}{\partial t} + \frac{\partial u_j \omega}{\partial x_j} = \frac{\gamma}{\nu_t} G - \beta \rho \omega^2 + \frac{\partial}{\partial x_j}\left[(\nu + \sigma_\omega \nu_t)\frac{\partial \omega}{\partial t}\right] + D \tag{4}$$

where turbulent viscosity is defined as:

$$\nu_t = \frac{\rho a_1 k}{max(a_1 \omega, \Omega F_2)} \tag{5}$$

2.3 Solver and numerical settings

The ground effect aerodynamics was simulated using the steady-state solver for the Reynolds averaged Navier-Stokes (RANS) equations closed by the k-ω SST model for turbulence. Under relaxation is applied for solution of steady RANS equations to increase convergence stability. Second order discretization schemes were used to solve momentum and pressure equations. All scalar variables are solved with the first order accuracy. The residuals for all the equations are allowed to reach a satisfactory convergence of $1/10000^{th}$ of the initial values.

2.4 Simulation results

In close proximity to the ground the airplane wing tip vortices are modified giving a reduced downwash contribution. This leads to increase in the lift force, reduction in the amount of induced drag, onset of the pitching down moment. For illustration purposes, Fig. 3 shows a pressure distribution on the CRM surfaces, the ground and in a far field cross-section at flight with altitude $h = 0.5\overline{c}$, angle of attack $\alpha = 8^\circ$ and bank angle $\phi = 4^\circ$. Note, the wing closer to the ground has a much weaker tip vortex than a similar vortex on the upper wing, which appears to be slightly elliptical. There is also zones with increased pressure on the ground under the wing and horizontal tail.

Transformations of the wing tip vortices in ground effect produce changes in the aerodynamic forces and moments acting on the aircraft. Fig.4 presents simulated dependencies for the lift, drag and also for the pitching, rolling and yawing moment coefficients. The ground effect increments in the aerodynamic loads increase with increase of the magnitude of the lift and strengthening the wing tip vortices and downwash outside of the ground. For example,

DOI: 10.13009/EUCASS2017-376

at $\alpha = 8^\circ$ and zero bank angle $\phi = 0$ the increase in the lift coefficient is $\triangle C_L = 0.08$, which is equivalent to increase on 11.2% (see Fig.4, top left plot). Further increase in the lift coefficient takes place at bank angle $\phi = 12^\circ$ - $\triangle C_L = 0.217$, which is equivalent to increase on 28.7% (see Fig.4, top right plot). The drag coefficient at bank angle $\phi = 12^\circ$ decreases, $\triangle C_D = -0.013$, this is equivalent to decrease on 11.8% (see Fig.4, top right plot).

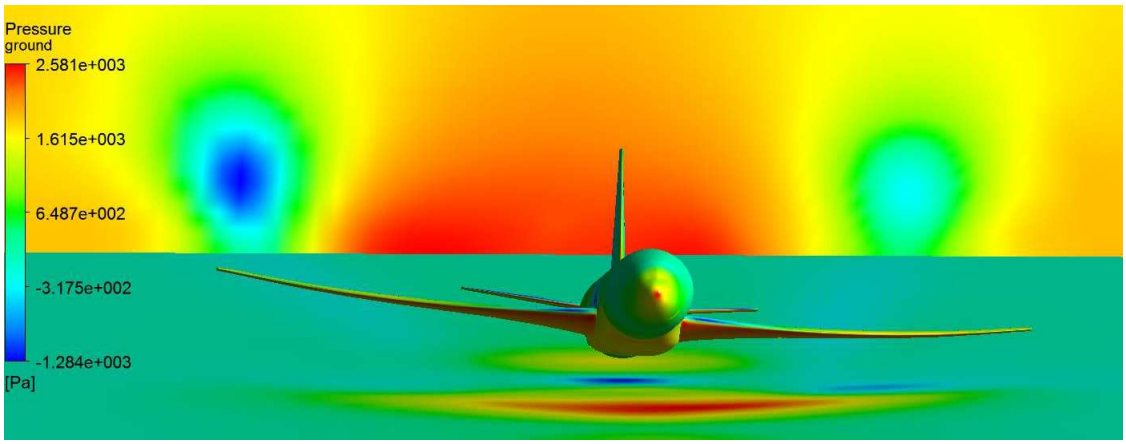

Figure 3: Pressure distribution on CRM surface, the ground and far field cross-section at $h = 0.5\bar{c}$, $\alpha = 8^\circ$ and $\phi = 4^\circ$.

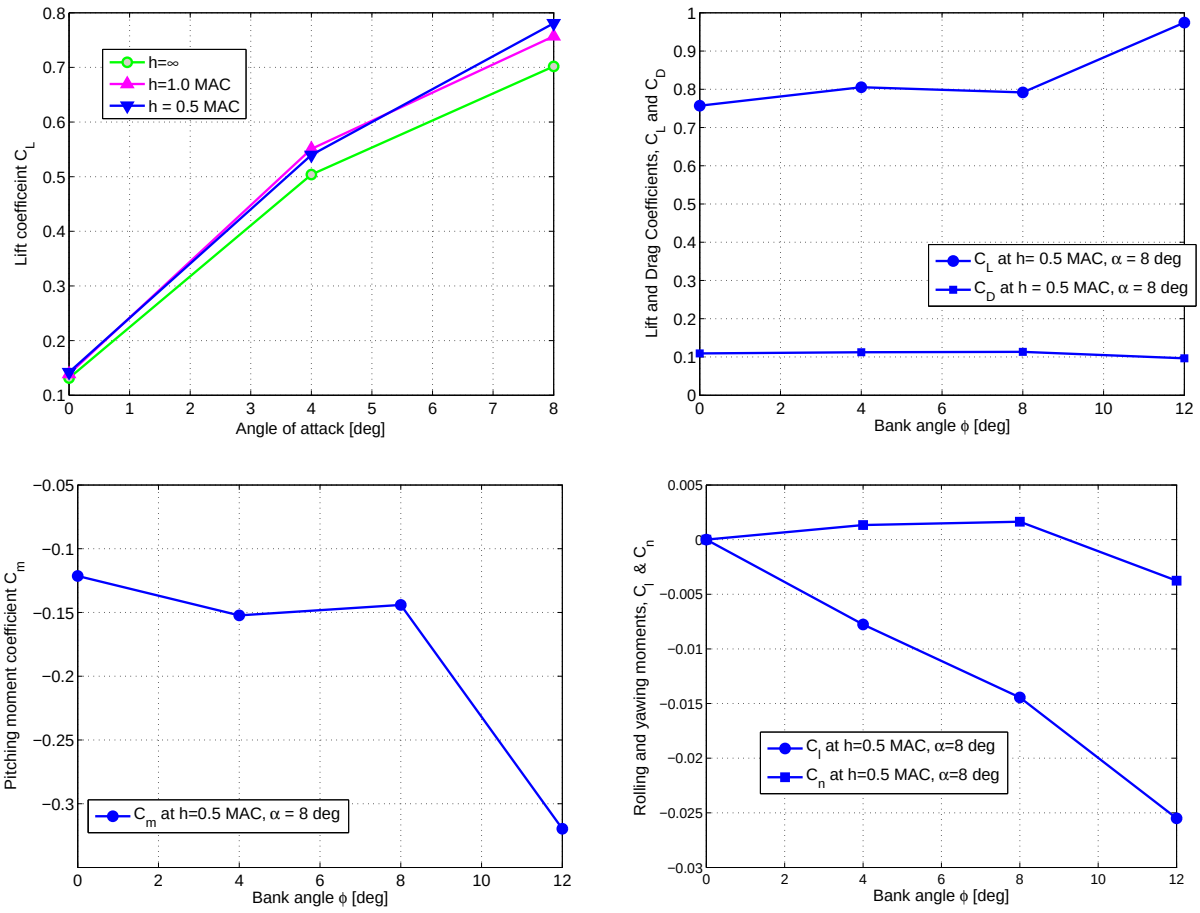

Figure 4: Effect of bank angle on aerodynamic coefficients C_L, C_D, C_m, C_l, C_n at $h = 0.5\bar{c}$, $\alpha = 8^\circ$.

The aerodynamic moments are also affected by the bank angle in close proximity to the ground. There is a significant pitching down effect at $\phi = 12^\circ$, i.e. $\triangle C_m = -0.198$ (see Fig.4, bottom left plot). The most important for

DOI: 10.13009/EUCASS2017-376

our objectives are the rolling and yawing moment dependencies on bank angle, shown in Fig.4, bottom right plot. The rolling moment coefficient C_l proportionally decreases with increase of bank angle ϕ, which is acting in a way as a stiff spring. The yawing moment coefficient increases with increase of bank angle until $\phi = 8°$, but decreases with the change of sign at $\phi = 12°$ (see Fig.4, bottom left plot).

3. Airplane lateral-directional dynamics in close proximity to the ground

The obtained in CFD simulations dependencies for the aerodynamic coefficients, presented in the previous section, have been used for modification of the full flight simulation model of a typical transport aircraft for conducting 6-DOF simulations in a level trimmed flight in close proximity to the ground. Trim and linearisation procedures have been applied to evaluate aircraft stability conditions and small amplitude modes of motion in the longitudinal and lateral-directional motion. Additionally, the impact of ground proximity on stability of the lateral-direction dynamics is addressed in this section with by the analysis of the linearised lateral-directional equations eigenvalues.

3.1 Lateral-directional equations

For evaluation of the airplane lateral-directional dynamics in close proximity to the ground the stability-axis lateral-directional equations are considered in the following vector-matrix form (see notations in[13]):

$$\begin{vmatrix} \dot{r} \\ \dot{\beta} \\ \dot{p} \\ \dot{\phi} \end{vmatrix} = \begin{bmatrix} N_r & N_\beta & N_p & N_\phi \\ -1 & Y_\beta & 0 & \frac{g}{V} \\ L_r & L_\beta & L_p & L_\phi \\ 0 & 0 & 1 & 0 \end{bmatrix} \begin{vmatrix} r \\ \beta \\ p \\ \phi \end{vmatrix} + \begin{bmatrix} N_{\delta_a} & N_{\delta_r} \\ 0 & 0 \\ L_{\delta_a} & L_{\delta_r} \\ 0 & 0 \end{bmatrix} \begin{vmatrix} \delta_a \\ \delta_r \end{vmatrix} \tag{6}$$

The new terms in the state matrix of equations (6) are $N_\phi = C_{n_\phi}(\bar{h})\frac{\rho V^2 S\, b}{2I_{zz}}$ and $L_\phi = C_{l_\phi}(\bar{h})\frac{\rho V^2 S\, b}{2I_{xx}}$. They represent the rolling and yawing accelerations induced by bank angle ϕ. The ground effect in this case is equivalent to a kind of "aerodynamic roll stiffness", which will tend to level the airplane above the runway.

In flight away from the ground, when $N_\phi = L_\phi = 0$, the lateral-directional modes are defined by the Roll-Dutch complex-conjugate eigenvalues $\lambda_{DR} = -\zeta \pm \omega_n \sqrt{(1-\zeta^2)}$, the roll subsidence eigenvalue λ_R and the spiral mode eigenvalue λ_S. It is reasonable to represent the ground effect on the eigenvalues in the form of a root-loci with a parameter connected with variation of the reduced flight altitude $\bar{h} = h/\bar{c}$.

3.2 Oscillatory Roll-Spiral mode in lateral-directional dynamics

The lateral-directional characteristic equation with account of ground effect can be represented in the following form:

$$(s-\lambda_S)(s-\lambda_R)(s^2 + 2\zeta\omega_n + \omega_n^2)_{DR} - L_\phi(s^2 + a_1 s + a_0)_{GE} = 0 \tag{7}$$

where

$$\begin{aligned} a_1 &= \frac{N_\phi}{L_\phi} L_r - N_r - \bar{Y}_\beta \\ a_0 &= N_\beta - \frac{N_\phi}{L_\phi} L_\beta + \left(N_r - \frac{N_\phi}{L_\phi} L_r \right) \bar{Y}_\beta \end{aligned} \tag{8}$$

Parameter L_ϕ varies from zero value in flight with no ground effect ($\bar{h} = \infty$) to its maximum value in close proximity to the ground ($\bar{h} = 0.5 \div 1.0$). The N_ϕ/L_ϕ ratio in expressions a_1 and a_2 (8) has a weak dependence on reduced altitude $\bar{h}$. So, with increase of parameter $|L_\phi|$ the eigenvalues will move on the complex plane from their initial values $\lambda_{DR} = -\zeta \pm \omega_n \sqrt{(1-\zeta^2)}$,$\lambda_R$ and λ_S towards the values defined by zeros z_1, z_2 of the second order polynomial equation $s^2 + a_1 s + a_0 = 0$ and one pair of eigenvalues will migrate to infinity. The location of zeros z_1 and z_2 depends on lateral directional coefficients in the expressions for a_1 and a_0 (8). These zeros can be located in the left half of the complex plane, being a complex-conjugate pair, or move to the right unstable half of the complex plane creating an opportunity for onset of oscillatory instability due to ground effect, when $a_1 < 0$. There is also a possibility for onset of aperiodical instability due to ground effect if $a_0 < 0$.

A full flight simulation model of a typical transport aircraft has been modified taking into account the aerodynamic dependencies presented in the previous section for the 6-DOF flight simulations in a level trimmed flight in close proximity to the ground. The eigenvalues of the linearised equations of motion are presented in Fig. 5 with variation of parameter $\bar{h}$. The eigenvalues root-loci shows significant transformation of the lateral-directional modes of motion.

DOI: 10.13009/EUCASS2017-376

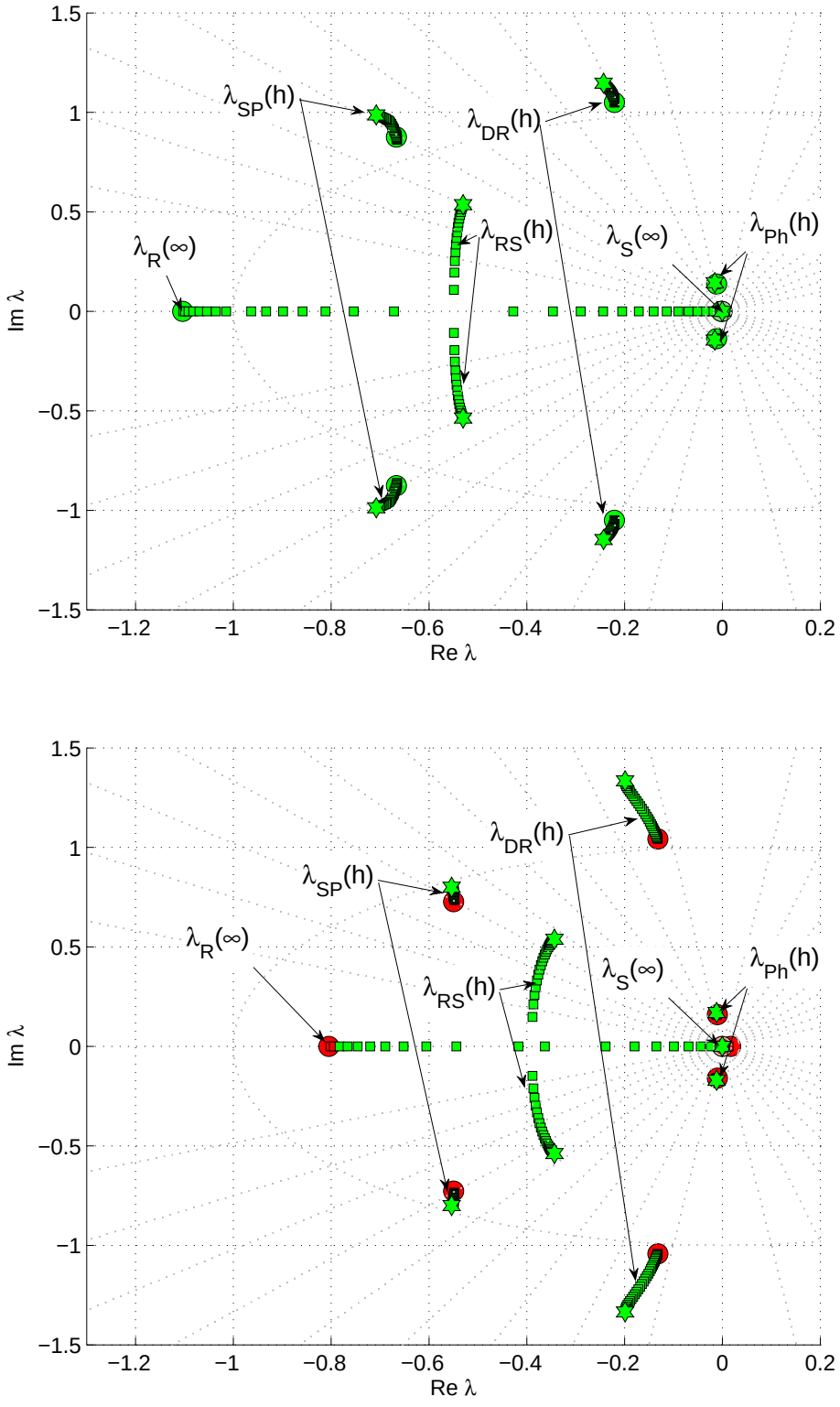

Figure 5: Root-loci of eigenvalues of the longitudinal and lateral-directional dynamics modes at different altitudes above the runway $h = 4.0\bar{c}$, $h = 2.5\bar{c}$ and $h = 1.0\bar{c}$, top plot - $\alpha = 3°$ and bottom plot - $\alpha = 8°$.

DOI: 10.13009/EUCASS2017-376

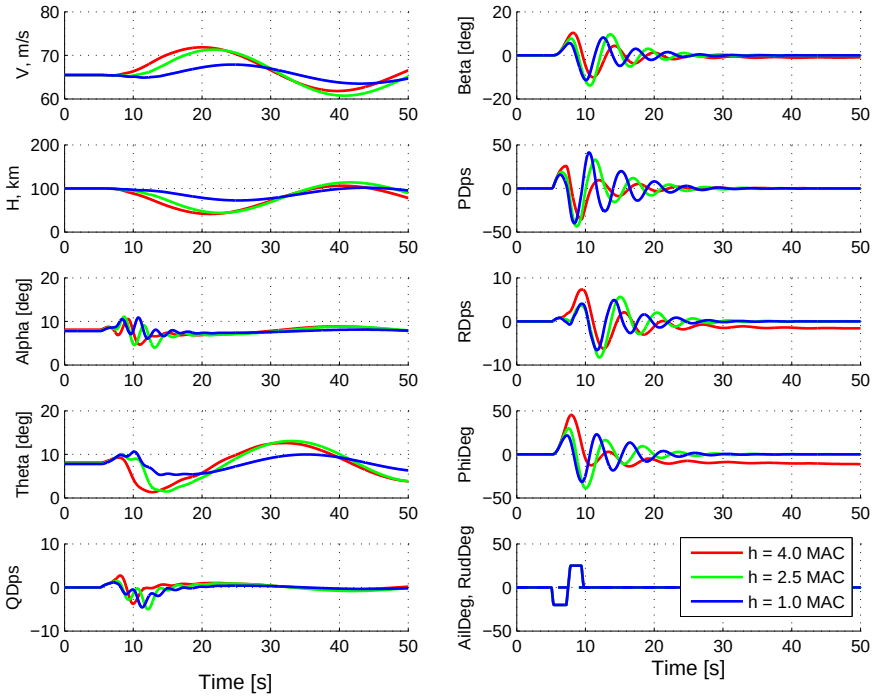

Figure 6: Airplane responses to doublet aileron control input $\delta_a = \pm 25^0$ at different altitudes above the runway obtained in 6-DOF simulation.

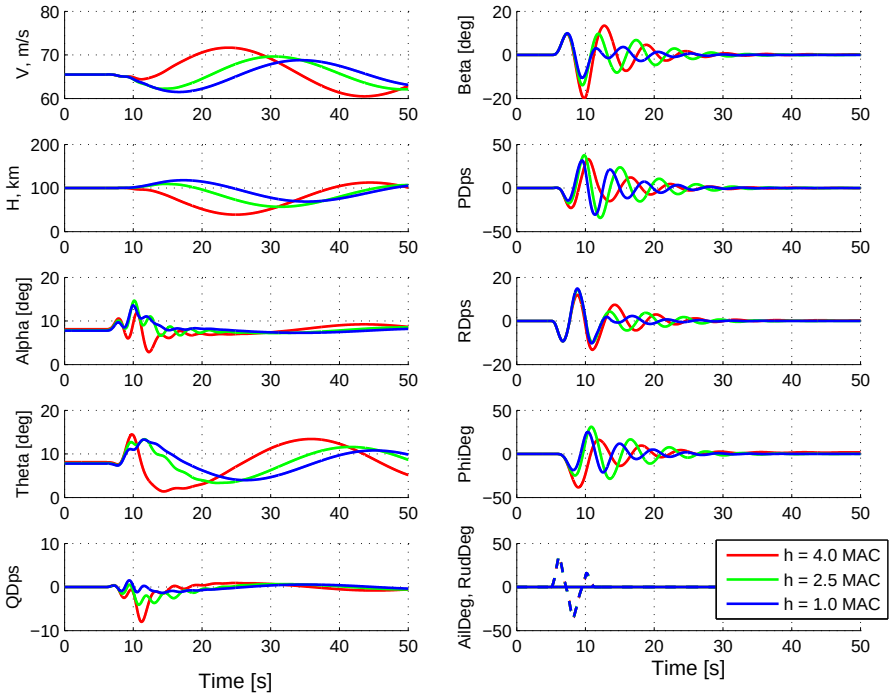

Figure 7: Airplane responses to doublet rudder control input $\delta_r = \pm 35^0$ at different altitudes above the runway obtained in 6-DOF simulation.

DOI: 10.13009/EUCASS2017-376

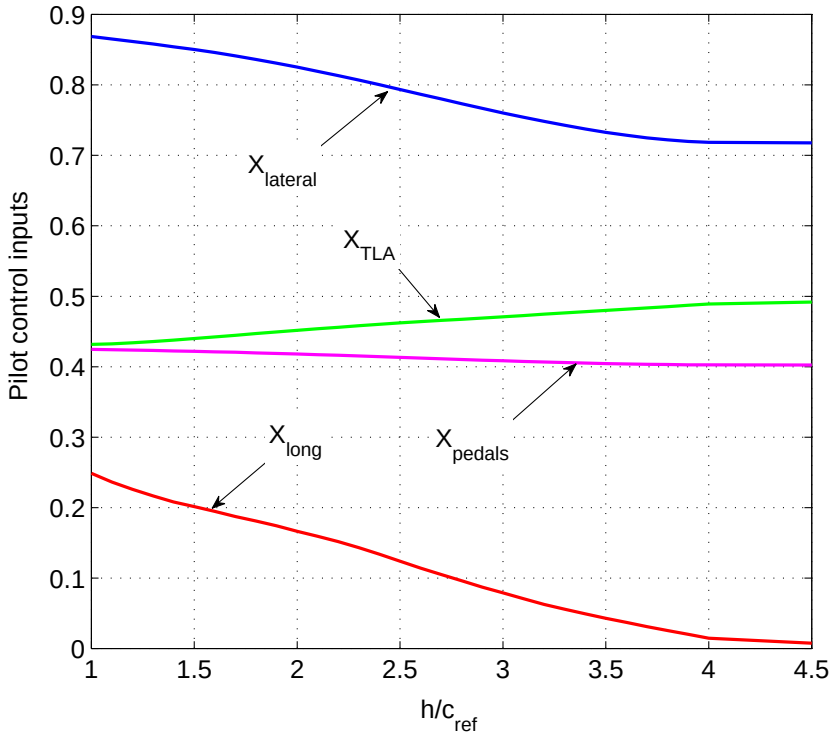

Figure 8: Trim control inputs required in landing approach with nonzero sideslip and bank angles ($\alpha = 8°$, $\beta = 10°$, $\phi = 4°$).

DOI: 10.13009/EUCASS2017-376

Table 1: Eigenvalues of Longitudinal and Lateral-Directional Dynamics Modes at $\alpha = 8°$.

Ground Effect	**Short period (SP)**	**Phugoid (Ph)**	**Roll (R)**	**Spiral (S)**	**Dutch Roll (DR)**
$h(\infty)$	$0.549 \pm 0.742i$	$-0.012 \pm 0.17i$	-0.8	-0.008	$-0.133 \pm 1.048i$
$h = 0.5\bar{c}$	$-0.554 \pm 0.8i$	$-0.012 \pm 0.17i$	$-0.344 + 0.538i$	$-0.344 - 0.538i$	$-0.2 \pm 1.335i$

[a]Roll and Spiral modes are merged in oscillatory Roll-Spiral (RS) mode

The roll subsidence and spiral eigenvalues in close proximity to the ground are merging creating the oscillatory Roll-Spiral mode with quite significant frequency $\omega_{RS} = 0.538 rad/s$ (see Fig.5(bottom plot $\alpha = 8°$)). Along with this change, the Dutch-roll eigenvalues increase frequency from the level of $\omega_D = 1.05 rad/s$ to $\omega_D = 1.34 rad/s$.

There is very little changes in the short-period longitudinal eigenvalues, λ_{SP} and practically no changes in the longitudinal phugoid mode, λ_{Ph}. In Table 1 the eigenvalues for the lateral-directional motion modes for flight at $h = \infty$ and $h = 1.0\bar{c}$ are presented for clarity showing a substantial transformation of the lateral-directional dynamics.

The new factor introduced in the performed eigenvalues analysis was the rolling and yawing moments depending on the airplane bank angle, which was equivalent to the "aerodynamic banking stiffness". This "aerodynamic stiffness" is strongly affecting the airplane controllability in close proximity to the ground. The airplane responses to aileron and rudder control inputs obtained in the 6-DOF flight simulation are shown in Figs.6 and 7, respectively. The airplane responses to pilot control inputs change in amplitudes and frequencies at low reduced altitudes $\bar{h} = h/\bar{c}$. This may lead to changes in handling qualities at low altitudes with effect on crosswind landing and onset of pilot induced oscillations.

In crosswind approach-and-landing the aircraft should fly with some nonzero sideslip angle to compensate side-wind. To fly a straight line along the runway the aircraft at the same time should have some non-zero sideslip and bank angles. Fig.8 shows the required control pilot inputs in trim flight with steady sideslip $\beta = 10°$, $\alpha = 8°$ and $\phi = 4°$. The control inputs are normalised with respect to maximum deflections. One can see that during landing significant retrimming is required in the longitudinal and lateral control channels and thrust control, and less sensitivity is shown in the directional channel.

4. Concluding remarks

The presented dynamic analysis of the lateral-directional motion modes and controllability during approach-and-landing shows the importance of the ground effect for the improved realism of piloted simulation and estimation of critical crosswinds. The introduced aerodynamic modelling allows improved pilot training on various types of flight simulators.

5. Acknowledgments

The authors appreciate discussions with test pilot Vladimir Biryukov and are grateful for his comments on crosswind approach-and-landing. His participation in preliminary piloted simulations helped to tune the aerodynamic model to produce realistic results.

DOI: 10.13009/EUCASS2017-376

References

[1] *Statistical Summary of Commercial Jet Airplane Accidents. World Wide Operations 1959-2015*. Aviation Safety, Boeing Commercial Airplanes, 2015.

[2] *Approach-and-landing Accident Reduction (ALAR) Briefing Note: 8.7 - Crosswind Landing*. Flight Safety Foundation, Flight Safety Digest, https://flightsafety.org/files/alar_bn8-7-crosswind.pdf, August-November 2000.

[3] M.R. Ahmed, T. Takasaki, and Y. Kohama. Aerodynamics of a naca 4412 airfoil in ground effect. *AIAA Journal*, 45:37–47, 2007.

[4] Erjie Cui and Xin Zhang. Ground effect aerodynamics. In *Encyclopedia of Aerospace Engineering*, 2010.

[5] Meredith C.W.Evans. Ground effect testing capabilities in the Filton $12' \times 10'$ low speed wind tunnel. *22nd International Congress of the Aeronautical Sciences, Harrogate, UK*, Paper ICAS-373, 27 Aug - 1 Sept 2000.

[6] G. Doig and T.J. Barber. Considerations for numerical modeling of inverted wings in ground effect. *AIAA Journal*, 49:2330–2333, 2011.

[7] https://aiaa-dpw.larc.nasa.gov/Workshop5/DPW5 geom.html, (last accessed 8 June 2017).

[8] https://commonresearchmodel.larc.nasa.gov/geometry/vertical-tail geometry, (last accessed 8 June 2017).

[9] S. Mahon and X. Zhang. Computational analysis of pressure and wake characteristics of an aerofoil in ground effect. *J. Fluids Eng. Trans. ASME*, 127:290–298, 2005.

[10] F. R. Menter. Improved two-equation k-ω turbulence models for aerodynamic flows. TM 103975, NACA, October 1992.

[11] OpenFOAM. The open source computational fuid dynamics toolbox. http://www.openfoam.com/, (last accessed 8 June 2017).

[12] R.W.Staufenbiel and U.-J.Schlichting. Stability of airplanes in ground effect. *Journal of Aircraft*, 25(4):289–294, April 1988.

[13] Robert F. Stengel. *Flight Dynamics*. Prinston University Press, 2004.

[14] X. Zhang and J. Zerihan. Edge vortices of a double-element wing in ground effect. *J. Aircr.*, 41:1127–1137, 2004.